



Cite this: *Polym. Chem.*, 2021, **12**,
2374

Received 19th January 2021,
Accepted 22nd March 2021

DOI: 10.1039/d1py00071c

rsc.li/polymers

We report the synthesis of cationic dendrons (1st and 2nd generations) with pendant alkyl chains of varying lengths (C₈, C₁₂, C₁₄), which are classified as cationic molecular umbrellas. In each case, the dendron surface moieties were functionalized with guanidine groups, which are fully protonated in aqueous media of pH 7.4, lending cationic character to the solute. We found that these compounds are potent membrane-disrupting antibacterial agents with dose-dependent hemolytic activities. Confocal microscopy confirmed the permeabilization of *E. coli* and *S. aureus* cell membranes. A pyrene emission assay confirms that the dendrons are unimolecularly solvated at the concentrations relevant to their antibacterial activity, although they do aggregate at higher concentrations in aqueous buffer. Most importantly, when we compare the activity of these guanidinium-functionalized umbrellas to our previously published data on ammonium-functionalized analogues, we found no significant benefits to guanidinium relative to the ammoniums. The antibacterial activities are similar in all cases tested, and the highest selectivity index was found in the ammonium series, which stands in contrast to many other classes of antibacterial agents for which guanidinylation is typically associated with enhanced activity and selectivity.

The alarming rise of antibiotic drug-resistant bacterial infections worldwide has generated much interest in alternative methods to stem the spread of harmful pathogens in the community and in the clinic.¹ A broad range of antimicrobial synthetic polymer chemistries, which were developed as inexpensive and synthetically scalable mimics of host defense peptides (HDPs), have shown potentially promising antibacterial activity and biocompatibility, both *in vitro* and *in vivo*.^{2,3} The mechanism of antibacterial activity is putatively mem-

brane disruption, although immunomodulatory effects may also play a role.⁴ Perhaps the most widely recognized molecular design principle for these materials is the concept of amphiphilic balance – judiciously optimized composition of cationic charge (which mediates electrostatic attraction to anionic lipids that are abundant in bacterial cell membranes) and hydrophobicity (which facilitates insertion into and disruption of the lipid bilayer).⁵ In this context, designing macromolecules with controlled spatial arrangement of these two elements remains a challenge at the forefront of the field. The notion of “facial amphiphilicity” argues that cationic charge and hydrophobicity ought to be predisposed to occupy opposite faces of the molecule, since the lipid bilayer is an approximately planar interface, at least locally, with anionic groups on one side and hydrophobic tails on the other.⁶ Many different approaches have been pursued in this vein, from random copolymers with conformational freedom to side chains containing facially-amphiphilic pendant units.^{7–10} Our own group recently developed the first example of a cationic “molecular umbrella” in which a long alkyl chain is attached to a dendron with cationic terminal groups.¹¹ In that first attempt, we identified a lead composition with potent antibacterial activity in the low $\mu\text{g mL}^{-1}$ concentration range and more than 1300-fold cell-type selectivity for bacteria *versus* mammalian cell membrane disruption.

The chemical structure of the cationic groups is known to be a major determinant of antibacterial and hemolytic activities in random copolymers.^{12,13} A popular choice for the cationic moiety is a protonated primary ammonium, which is mostly cationic in neutral aqueous media by virtue of protonation.¹⁴ Primary ammoniums, which are selected because they mimic lysine residues that are abundant in HDPs, often show better cell-type selectivity when directly compared to the more conventional choice of quaternary ammonium salt (QAS) groups.¹⁵ Furthermore, guanidinium moieties are also a popular choice, because they mimic arginine residues also found in HDPs and are known to bind more strongly to phospholipid headgroups *via* a combination of coulombic attrac-

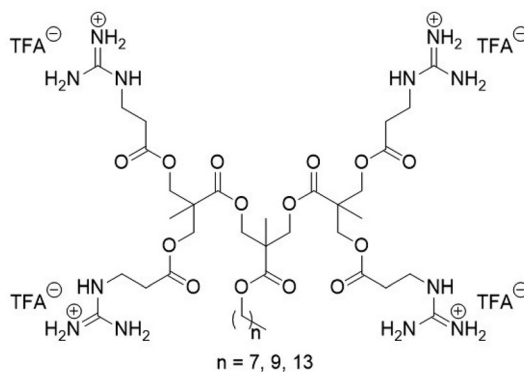
^aSchool of Biomedical Engineering, Shanghai Jiao Tong University, Shanghai, 200030, China

^bMaterials Science and Engineering, Rensselaer Polytechnic Institute, 110 8th St, Troy, NY, 12180, USA. E-mail: palere@rpi.edu

† Electronic supplementary information (ESI) available. See DOI: 10.1039/d1py00071c

tion and bidentate hydrogen bonding interactions.¹⁶⁻¹⁹ These examples in the literature have shown enhancement of antibacterial activity in direct comparison between ammonium- and guanidinium-functionalized, although comparable^{20,21} or reduction²² of antimicrobials were reported after the guanidinylation of certain HDP-mimetic structures. Thus, we questioned whether converting our ammonium-functionalized cationic molecular umbrellas (described above) to guanidinium variants could further enhance their already outstanding activity.

Guanidinium-functionalized cationic molecular umbrellas were prepared by minor modifications to our previously published route (Scheme 1).¹¹ Detailed procedures and characterization data are provided in the ESI.† Briefly, β -alanine was guanidinylated using diBoc-protected *S*-methylisothiourea in methanol with K_2CO_3 and 4-dimethylaminopyridine (DMAP). Dendrons of 2,2-bis(hydroxymethyl)propionic acid (bis-MPA) containing pendant hydroxyl surface groups, as well as a long hydrophobic chain attached to the core, were then coupled to the Boc-protected guanidino propanoic acid *via* standard *N,N'*-dicyclohexylcarbodiimide (DCC)/DMAP chemistry, and finally were deprotected with neat trifluoroacetic acid (TFA). Synthesis of the variants containing C_8 , C_{10} , and C_{14} hydrophobic handles was successful for the 1st and 2nd generation dendrons. Attempts to functionalize the 3rd generation examples led to less than quantitative surface group conversion, which stalled at less than ~6 out of 8 functionalized surface groups in the best case. Moreover, these samples contained an intractable impurity that was challenging to remove. Presumably, the difficulty can be ascribed to the bulkiness of the doubly Boc-protected guanidine group, which crowds out the remaining unreacted -OH moieties presented on the dendron surface. Thus, we proceeded to characterize the 1st and 2nd generation dendrons as an initial screen. As our main goal of this work was to directly compare dendrons that only differ in terms of the source of cationic charge (guanidium *versus* ammonium), the question of how to obtain the 3rd generation dendron was considered unnecessary to that end, and was thus relegated such effort to our future work. The chemical structure of the



Scheme 1 Chemical structure of the G2 amphiphilic cationic molecular umbrellas that display guanidinium groups on the dendron surface and a long alkyl chain as the hydrophobic tail component.

2nd generation dendrons with cationic guanidinium groups is given in Scheme 1.

Compounds in this work are denoted as C_nG_x where n is the number of carbons in the linear alkyl chain and x is the generation number of the dendron. For example, $C_{14}G_2$ is the 2nd generation dendron attached to a $-C_{14}H_{29}$ alkyl chain. The antimicrobial and hemolytic activities, along with characterization data, of all compounds in this study are listed in Table 1.

The antibacterial activities observed in the 1st generation dendron series, for which each compound contains just two protonated (cationic) guanidinium groups, are well in line with expectations based on the amphiphilic balance framework. While the C₈G₁ compound showed weak activity (Minimum Inhibitory Concentration (MIC) values of 250 and 500 $\mu\text{g mL}^{-1}$ for *E. coli* and *S. aureus*, respectively), increasing the hydrophobicity monotonically enhances antimicrobial potency. For example, as the alkyl chain length increased to C₁₀ chains, the antibacterial activity is enhanced (MIC 62.5 $\mu\text{g mL}^{-1}$ for both strains) and further increasing to C₁₄ results in potent antimicrobial activity (MIC 7.8 $\mu\text{g mL}^{-1}$). Hemolytic activities against sheep red blood cells (RBC, MP Biomedicals) follow a similar trend, with hemolysis observed at lower concentrations for the more hydrophobic compounds. In Table 1, we list the Hemolytic Concentration 50% (HC₅₀) values, which are widely considered the characteristic hemolytic concentrations (although some authors express a preference for the more conservative Hemolytic Concentration 10% (HC₁₀) values). We include the entire hemolysis dose-response curves and curve fits to the modified Hill equation, in the ESI† document so that any characteristic value one prefers may be extracted. In terms of selectivity between bacterial cells and RBCs, the 1st generation series is categorized as biocidal because the antibacterial and hemolytic activities are of similar magnitude in each case. In the 2nd generation series, for which four cationic guanidinium groups are displayed on each dendron, the trends for antibacterial activity are nearly the same as the 1st generation, but the hemolytic activities are less severe. The

Table 1 Antibacterial (Minimum Inhibitory Concentration, MIC) and hemolytic activity (Hemolytic Concentration 50%, HC₅₀), and critical micelle concentrations (CMC), for the guanidine-functionalized cationic molecular umbrellas

| Cmpd | Gen. | C _n | MW (g mol ⁻¹) | MIC (µg mL ⁻¹) | | HC ₅₀ (µg mL ⁻¹) RBC ^c | CMC (µg mL ⁻¹) |
|--------------------------------|------|----------------|------------------------------|-----------------------------|-------------------------------|--|-------------------------------|
| | | | | <i>E. coli</i> ^a | <i>S. aureus</i> ^b | | |
| C ₈ G ₁ | G1 | 8 | 701 | 250 | 500 | 438 | >10 000 |
| C ₁₀ G ₁ | | 10 | 729 | 62.5 | 62.5 | 279 | 9640 |
| C ₁₄ G ₁ | | 14 | 785 | 7.8 | 7.8 | 23 | 1170 |
| C ₈ G ₂ | G2 | 8 | 1387 | 1000 | 250 | 1553 | >10 000 |
| C ₁₀ G ₂ | | 10 | 1415 | 62.5 | 62.5 | 327 | 1633 |
| C ₁₄ G ₂ | | 14 | 1471 | 7.8 | 7.8 | 117 | 201 |

^a *E. coli* strain ATCC 25922. ^b *S. aureus* strain ATCC 25923. ^c Sheep red blood cells (RBC) obtained from MP biomedicals.

compound $C_{14}G_2$ displayed the highest selectivity index in the series, albeit a relatively modest value ($HC_{50}/MIC = 15$).

Analysis of aggregation in aqueous media was performed using a pyrene emission assay in the same manner as previously described.¹¹ Here, we define the critical micelle concentration (CMC) as the inflection point on the sigmoidal dose-response curves of I_1/I_3 versus dendron concentration. Two observations are clear in the dataset. First, as expected, increasing hydrophobicity leads to aggregation in aqueous media at lower concentrations. Second, we also find in all cases that the CMC is higher than both the MIC and HC_{50} values for a given example compound. Thus, we suggest that the active species is indeed individually solvated at the concentrations required to exert membrane activity, rather than an aggregate or micelle assembled from these cationic surfactant molecules in solution. Plots are given in the ESI.†

Confocal laser scanning microscopy was performed on *E. coli* and *S. aureus* treated with $C_{14}G_2$ at concentrations of 1× and 4× MIC with SYTO-9 and Propidium Iodide (PI) staining. The green SYTO9 stains all cells and the red PI only emits red when the membrane barrier function has been compromised. We find that untreated control *E. coli* sample shows the bacterial cells with smooth rod-like shape stained extensively with the green SYTO9, but with no significant red PI staining, indicative of all live cells (Fig. 1A and B). In contrast, treated *E. coli* cells showed a diminished green emission intensity with concomitant bright red emission, indicative of cell membrane permeabilization (Fig. 1C and D).

To further corroborate the notion of a membrane disruption mechanism with higher resolution images we also examined fixed *E. coli* cells by Scanning Electron Microscopy (SEM) as shown in Fig. 1E. The untreated control sample (inset in Fig. 1E) reveals the expected intact rod-shaped morphology of the *E. coli* cell. In contrast, the *E. coli* suspension incubated with 32 $\mu\text{g mL}^{-1}$ of $C_{14}G_2$ shows gross disruption of cell shape, which is consistent with a direct mode of action against bacterial membranes.

Finally, we sought to directly compare the guanidinium-functionalized dendrons in this work to the previously

described ammonium-functionalized dendrons¹¹ of our recent paper. Importantly, these structures are chemically identical except for the identity of the cationic group. To that end, we prepared a log-log plot of MIC versus HC_{50} with guidelines to represent regions of constant selectivity index (SI, HC_{50}/MIC). From these data, we do not observe a clear or universal preference for ammonium or guanidinium surface groups on these cationic molecular umbrella type dendrons, at least for dendron generations 1 and 2. Although the trends are generally similar in both cases, there are some instances where the identity of the cationic charge appears to have a pronounced impact. For example, in the case of $C_{10}G_2$, the SI is nearly an order of magnitude higher when the cationic groups are ammonium instead of guanidinium groups. In contrast, C_8G_1 and C_8G_2 both showed better SI for guanidinium, relative to ammonium groups, by about a factor of 3 (Fig. 2).

In conclusion, this structure–activity relationship study revealed certain examples of biological activity in cationic molecular umbrellas that depends somewhat on the identity of the cationic groups (ammonium vs. guanidinium). However, guanidinylation of amines does not appear to universally enhance antibacterial activity or cell-type selectivity in the cationic umbrella design platform explored here. Indeed, another study from our laboratory, regarding the activity of photodynamic antibacterial oligothiophenes, also found that guanidinylation had only modest effects on activity.²¹ Although much literature has been devoted to the development of guanidinium-rich antibacterial polymers as a method to enhance activity relative to ammonium-rich analogues, we have found that the effect is not necessarily universal. Overall, the highest cell-type selectivity in this small library screening effort was identified as $C_{10}G_2$ with ammonium groups displayed on the dendron surface. In consideration of the contradictory effects of guanidinylation in other polymer systems, we suggest that such difference may result from the specific polymer structures. For molecular umbrellas, more effort will be focused on the structure–antibacterial behavior to better understand the difference in ammonium vs. guanidinium functionalization in future investigations. Based on the available literature regard-

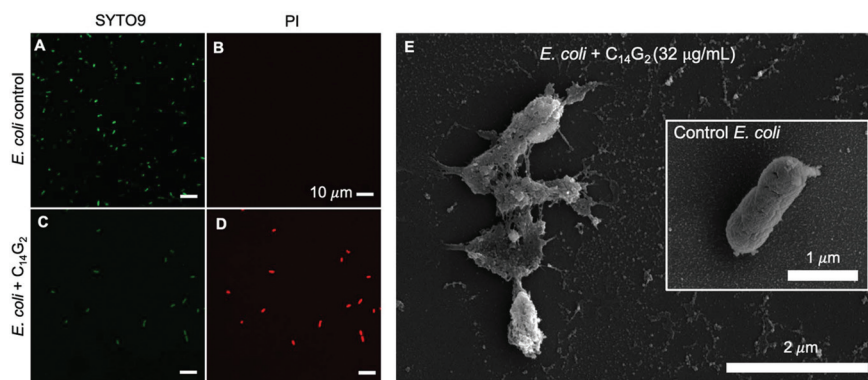


Fig. 1 Confocal laser scanning microscopy images of (A and B) *E. coli* in PBS and (C and D) *E. coli* exposed to $C_{14}G_2$ at 32 $\mu\text{g mL}^{-1}$ and (E) Scanning Electron Microscopy (SEM) images of *E. coli* exposed to $C_{14}G_2$ at 32 $\mu\text{g mL}^{-1}$ compared to (inset) *E. coli* alone, both after fixation.

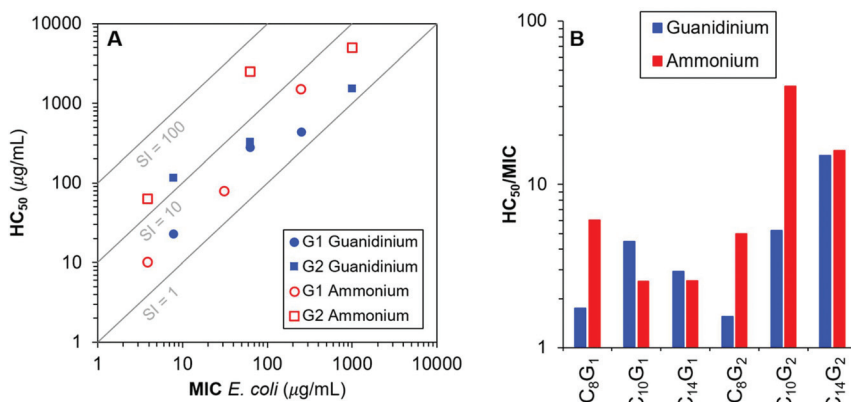


Fig. 2 (A) log–log Ashby plot of hemolytic activity against sheep red blood cells versus antimicrobial activity against *E. coli* and (B) bar chart of selectivity index, HC_{50}/MIC , for the 1st and 2nd generation dendrons as a function of the chemical structure of their cationic charges.

ing synthetic mimics of cell-penetrating peptides,²³ these guanidinium containing molecular umbrellas should also be evaluated for their cytotoxicity and cell transfection efficiencies in future studies.

Conflicts of interest

AC and EFP are co-inventors on a provisional patent application entitled "Antimicrobial Compositions Including Janus Dendrons" related to the structures shown in this work.

Acknowledgements

This work was supported in part by the National Science Foundation (Award #1653418). The donors of the American Chemical Society Petroleum Research Fund are gratefully acknowledged (57806-DNI7).

References

- 1 H. W. Boucher, Bad Bugs, No Drugs 2002-2020: Progress, Challenges, and Call to Action, *Trans. Am. Clin. Climatol. Assoc.*, 2020, **131**, 65–71.
- 2 C. Ergene, K. Yasuhara and E. F. Palermo, Biomimetic Antimicrobial Polymers: Recent Advances in Molecular Design, *Polym. Chem.*, 2018, **9**, 2407–2427, DOI: 10.1039/c8py00012c.
- 3 R. W. Scott and G. N. Tew, Mimics of Host Defense Proteins; Strategies for Translation to Therapeutic Applications, *Curr. Top. Med. Chem.*, 2016, **17**(5), 576–589, DOI: 10.2174/1568026616666160713130452.
- 4 K. A. Brogden, Antimicrobial Peptides: Pore Formers or Metabolic Inhibitors in Bacteria?, *Nat. Rev. Microbiol.*, 2005, 238–250, DOI: 10.1038/nrmicro1098.
- 5 E. F. Palermo, K. Lienkamp, E. R. Gillies and P. J. Ragogna, Antibacterial Activity of Polymers: Discussions on the Nature of Amphiphilic Balance, *Angew. Chem.*, 2019, **131**(12), 3728–3731, DOI: 10.1002/ange.201813810.
- 6 G. N. Tew, D. Liu, B. Chen, R. J. Doerksen, J. Kaplan, P. J. Carroll, M. L. Klein and W. F. Degrado, De Novo Design of Biomimetic Antimicrobial Polymers, *Proc. Natl. Acad. Sci. U. S. A.*, 2002, **99**(8), 5110–5114, DOI: 10.1073/pnas.082046199.
- 7 K. Lienkamp, A. E. Madkour, A. Musante, C. F. Nelson, K. Nüsslein and G. N. Tew, Antimicrobial Polymers Prepared by ROMP with Unprecedented Selectivity: A Molecular Construction Kit Approach, *J. Am. Chem. Soc.*, 2008, **130**(30), 9836–9843, DOI: 10.1021/ja801662y.
- 8 B. P. Mowery, S. E. Lee, D. A. Kissounko, R. F. Epand, R. M. Epand, B. Weisblum, S. S. Stahl and S. H. Gellman, Mimicry of Antimicrobial Host-Defense Peptides by Random Copolymers, *J. Am. Chem. Soc.*, 2007, **129**(50), 15474–15476, DOI: 10.1021/ja077288d.
- 9 Z. Zhou, C. Ergene, J. Y. Lee, D. J. Shirley, B. R. Carone, G. A. Caputo and E. F. Palermo, Sequence and Dispersity Are Determinants of Photodynamic Antibacterial Activity Exerted by Peptidomimetic Oligo(Thiophene)S, *ACS Appl. Mater. Interfaces*, 2019, **11**(2), 1896–1906, DOI: 10.1021/acsami.8b19098.
- 10 M. A. Rahman, M. Bam, E. Luat, M. S. Jui, M. S. Ganewatta, T. Shokfai, M. Nagarkatti, A. W. Decho and C. Tang, Macromolecular-Clustered Facial Amphiphilic Antimicrobials, *Nat. Commun.*, 2018, **9**, 5231, DOI: 10.1038/s41467-018-07651-7.
- 11 A. Chen, A. Karanastasis, K. R. Casey, M. Necelis, B. R. Carone, G. A. Caputo and E. F. Palermo, Cationic Molecular Umbrellas as Antibacterial Agents with Remarkable Cell-Type Selectivity, *ACS Appl. Mater. Interfaces*, 2020, **12**(19), 21270–21282, DOI: 10.1021/acsami.9b19076.
- 12 E. F. Palermo and K. Kuroda, Chemical Structure of Cationic Groups in Amphiphilic Polymethacrylates Modulates the Antimicrobial and Hemolytic Activities, *Biomacromolecules*, 2009, **10**(6), 1416–1428, DOI: 10.1021/bm900044x.

13 E. F. Palermo, S. Vemparala and K. Kuroda, Cationic Spacer Arm Design Strategy for Control of Antimicrobial Activity and Conformation of Amphiphilic Methacrylate Random Copolymers, *Biomacromolecules*, 2012, **13**(5), 1632–1641, DOI: 10.1021/bm300342u.

14 M. A. Gelman, B. Weisblum, D. M. Lynn and S. H. Gellman, Biocidal Activity of Polystyrenes That Are Cationic by Virtue of Protonation, *Org. Lett.*, 2004, **6**(4), 557–560, DOI: 10.1021/ol036341+.

15 E. F. Palermo and K. Kuroda, Structural Determinants of Antimicrobial Activity in Polymers Which Mimic Host Defense Peptides, *Appl. Microbiol. Biotechnol.*, 2010, **87**(5), 1605–1615, DOI: 10.1007/s00253-010-2687-z.

16 K. E. S. Locock, Bioinspired Polymers: Antimicrobial Polymethacrylates, *Aust. J. Chem.*, 2016, **69**(7), 717–724, DOI: 10.1071/CH16047.

17 K. E. S. Locock, T. D. Michl, J. D. P. Valentin, K. Vasilev, J. D. Hayball, Y. Qu, A. Traven, H. J. Griesser, L. Meagher and M. Haeussler, Guanylated Polymethacrylates: A Class of Potent Antimicrobial Polymers with Low Hemolytic Activity, *Biomacromolecules*, 2013, **14**(11), 4021–4031, DOI: 10.1021/bm401128r.

18 D. Liu, S. Choi, B. Chen, R. J. Doerkens, D. J. Clements, J. D. Winkler, M. L. Klein and W. F. DeGrado, Nontoxic Membrane-Active Antimicrobial Arylamide Oligomers, *Angew. Chem., Int. Ed.*, 2004, **43**(9), 1158–1162, DOI: 10.1002/anie.200352791.

19 M. Arias, K. Piga, M. Hyndman and H. Vogel, Improving the Activity of Trp-Rich Antimicrobial Peptides by Arg/Lys Substitutions and Changing the Length of Cationic Residues, *Biomolecules*, 2018, **8**(2), 19, DOI: 10.3390/biom8020019.

20 E. Kohn, D. Shirley, L. Arotsky, A. Picciano, Z. Ridgway, M. Urban, B. Carone and G. Caputo, Role of Cationic Side Chains in the Antimicrobial Activity of C18G, *Molecules*, 2018, **23**(2), 329, DOI: 10.3390/molecules23020329.

21 Z. Zhou, C. Ergene and E. F. Palermo, Guanidinium-Functionalized Photodynamic Antibacterial Oligo (Thiophene)S, *MRS Adv.*, 2019, **4**(59–60), 3223–3231, DOI: 10.1557/adv.2019.359.

22 S. E. Exley, L. C. Paslay, G. S. Sahukhal, B. A. Abel, T. D. Brown, C. L. McCormick, S. Heinhorst, V. Koul, V. Choudhary, M. O. Elasri and S. E. Morgan, Antimicrobial Peptide Mimicking Primary Amine and Guanidine Containing Methacrylamide Copolymers Prepared by Raft Polymerization, *Biomacromolecules*, 2015, **16**(12), 3845–3852, DOI: 10.1021/acs.biomac.5b01162.

23 B. M. deRonde and G. N. Tew, Development of Protein Mimics for Intracellular Delivery, *Biopolymers*, 2015, **104**(4), 265–280, DOI: 10.1002/bip.22658.